Journal of Materials Chemistry C

Accepted Manuscript

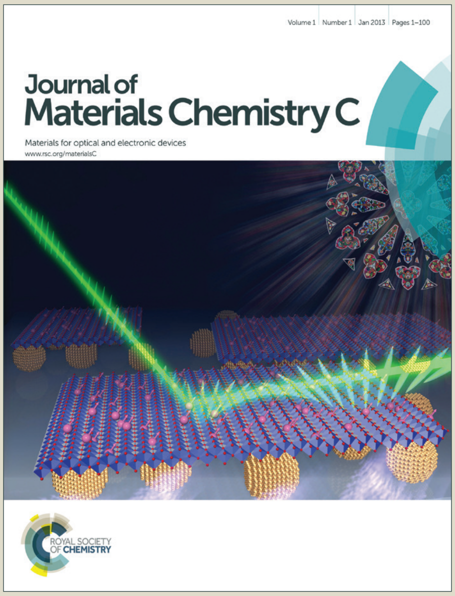

ROYAL SOCIETY OF CHEMISTRY

www.rsc.org/materialsC

Copolyfluorenes Containing Partially Hydrolyzed Phosphonate Pendant Groups: Synthesis, Characterization and Application as Electron Injection Layer for Enhanced Electroluminescence of PLEDs

Chia-Shing Wu, Chen-Yi Chou and Yun Chen*

Department of Chemical Engineering, National Cheng Kung University, Tainan, Taiwan

*Corresponding author: yunchen@mail.ncku.edu.tw

Abstract

Balance in charges injection is crucial to improve device performance of polymer light-emitting diodes (PLEDs); however, hole injection is much easy than electron injection in most PLEDs. We synthesized copolyfluorenes containing pendant phosphonate groups (**PF-EP**) or partially hydrolyzed phosphonate groups (**PF-EPK**) and successfully applied them as electron injection layer (EIL) in PLEDs to significantly enhance device performance. Multilayer PLEDs [ITO/PEDOT:PSS/Superyellow (SY)/**PF-EP**+**PF-EPK**/Al] were readily fabricated using blends of **PF-EPK** and **PF-EP** as EIL by solution process. The device with **PF-EP** doped with 2.5% **PF-EPK** as EIL exhibited the best performance. The device performance were enhanced to 12052 cd/m^2, 3.62 cd/A and 1.38 lm/W, respectively, from 725 cd/m^2, 0.16 cd/A and 0.05 lm/W of non-EIL device. The performance enhancement has been attributed to improved electron injection which has been confirmed by the raise in open-circuit voltage (V_{oc}) obtained from photovoltaic measurements. The results indicate that **PF-EPK** is a promising electron-injection material for optoelectronic devices with high work function Al cathode.

Introduction

Polymer light-emitting diodes (PLEDs)[1-3], conjugated polymers (CPs) based organic electronic devices, have attracted considerable attention for more than two decades. Owning to their advantages of easy fabrication by spin-coating or ink-jet printing technique via solution processing and lower production cost, especially for the large-size devices. Now it is well known that high-efficiency PLEDs need a multilayer device structure to achieve efficient and balanced electron and hole injection and transport from metal cathode and anode[4, 5]. This results in commonly used multilayer device structures, including the transparent conducting indium tin oxide (ITO) anode, hole transport/injection layer (HTL/HIL), emitting layer (EML), electron transport/injection layer (ETL/EIL), and metal cathode. However, the solution process brings a big challenge for most of the commonly used emitting and transport materials have similar solubility in common organic solvents, this may cause erosion of the preceding layers during multilayer integration[6].

Crosslinkable HTL and EML materials have been developed to form robust films with excellent solvent resistance after thermo- or photo-crosslinking[7-9]; however, the commercial material, poly(3,4-ethylene-dioxythiophene): poly(styrene sulfonic acid) (PEDOT:PSS), has been widely used in PLEDs to improve hole injection and transport successfully[10]. For most CPs, electron injection is more difficult than hole injection for the high energy barrier between the EML and the metal cathode[11]. Therefore, efficient injection of electrons from the cathode to EML is an essential factor to improve the device efficiency.

Among the typical conjugated fluorescent materials we investigated,[12] polyfluorenes (PFs) derivatives show good thermal stability and exhibit good photoluminescence (PL) efficiency. Recently, polyfluorene-based water/alcohol soluble conjugated polymers (WSCPs)[6] with totally orthogonal solubility with the commonly used EML were demonstrated to be good EIL materials for PLEDs. The polar groups on their side chains can form interfacial dipoles between the EML and metal cathode to enhance electron injection. The unique solubility and excellent injection ability of these materials offer the possibility to improve electron injection and conduction by doping them with water-soluble alkali or alkaline earth-metal salts, which have been successfully used as n-dopants in PLEDs[10]. Although doping inorganic salts (LiF, Cs_2CO_3 and Li_2CO_3)[10, 13, 14] in EILs is an effective method to further improve electron injection property, the moisture-absorbing and small molecular inorganic salts are severely aggregated with increasing blending concentration. The morphology of polymer films is another crucial factor that affects the performance of devices[10].

In this study, we take advantage of the widely used WSCPs material, polyfluorenes with phosphonate ester (**PF-EP**), and further develop partially hydrolyzed phosphonate groups with potassium ion (**PF-EPK**) as the dopant to cooperate with **PF-EP** in EIL to enhance the efficiency of the devices. **PF-EPK** not only increases the electron injection from the metal cathode to EIL but also is applied as electron transporting moieties. In addition, partially hydrolyzed **PF-EPK** preserved **PF-EP** unit is more compatible with **PE-EP** due to their similar chemical structures and well dispersed in EIL because of polymer chain extension.

Experimental Section

Measurement and Characterization

All synthesized compounds were identified by ^1H NMR and elemental analysis (EA), and polymers were also identified by ^{31}P NMR. The ^1H and ^{31}P NMR spectra were recorded on a Bruker AMX-600 MHz FT-NMR, with the chemical shifts reported in ppm using tetramethylsilane (TMS) as an internal standard. The elemental analysis was carried out on a Heraus CHN-Rapid elemental analyzer. The thermogravimetric analysis (TGA) was performed under a nitrogen atmosphere using a PerkinElmer TGA-7 thermal analyzer at a heating rate of 10 °C/min. Cyclic voltammograms were measured with a voltammetric apparatus (model CV-50W from BAS) equipped with a three-electrode cell. The cell was made up of a polymer-coated glassy carbon as the working electrode, an Ag/AgCl electrode as the reference electrode, and a platinum wire as the auxiliary electrode. The electrodes were immersed in acetonitrile containing 0.1 M $(n\text{-}Bu)_4NClO_4$ as electrolyte. The energy levels were calculated using the ferrocene (FOC) value of -4.8 eV with respect to vacuum level, which is defined as zero. Atomic force microscope (AFM), equipped with a Veeco/Digital Instrument Scanning Probe Microscope (tapping mode) and a Nanoscope III controller, was used to examine the morphology of polymer film surfaces and to estimate their root-mean-square (RMS) roughness.

PLED Fabrication and Characterization

The water/alcohol-soluble copolyfluorenes were used as an electron-injecting layer in multilayer polymer light-emitting diodes (PLEDs), with a device structure of ITO/PEDOT:PSS (25 nm)/SY (75 nm)/EIL (40 nm)/Al (80 nm), were fabricated by the solution processes for the investigation of optoelectronic characteristics. Patterned indium tin oxide (ITO)-coated glass substrates as the anode was cleaned in ultrasonic baths with neutral reiniger/deionized water (1:3 v/v) mixture, deionized water, acetone, isopropanol, and deionized water. A surface treatment was carried out by UV-ozone. The hole injection layer (PEDOT:PSS, HIL, Bayer) was spin-coated onto the ITO at a thickness of 25 nm and baked at 150 ^{o}C for 15 min on a hot plate under air. A yellow-light-emitting polyphenylene vinylene (PPV) derivatives (SY, Merck) dissolved in toluene was spin-coated onto the HIL layers to obtain a thickness of 75 nm, and was subsequently baked at 65 °C for 25 min to remove the residual solvent. A 0.1 wt% mixture solvent of **PF-EPK** and **PF-EP** in methanol/water (19:1 v/v) was spin-coated onto the emitting layer as an electron-injecting layer and baked at 50 °C for 30 min. The aluminum (80 nm) was deposited as the cathode by thermal evaporation at about 1×10^{-6} Torr. The electroluminescence (EL) spectra and current-luminance-voltage (I-L-V) characteristics of the devices were recorded using a combination of a Keithley power source (model 2400) and an Ocean Optics usb2000 fluorescence spectrophotometer. Current efficiency and luminous power efficiency were calculated from the I-L-V characteristics. The photovoltaic measurement was performed under the illumination supplied by a Thermo Oriel 150W solar simulator AM 1.5G. The fabrication of the devices was done in ambient conditions, with the following performance tests conducted in a glove-box filled with nitrogen.

Material Synthesis

All reagents and solvents obtained from Acros, Aldrich, Showa, and Lancaster were directly used without further purification except specifically notified.

Poly[9,9-bis(5'-diethoxylphosphorylpentyl)-fluorene] (PF-EP)

Aqueous K_2CO_3 (1 M, 0.5 ml) and DMF (3.0 ml) were added to a mixture of monomer **2** and **3** with $Pd(PPh_3)_4$ (1 mol%) under nitrogen and refluxed for 2 days with vigorous stirring. The resulting solution was dialyzed against water and methanol using cellulose membrane (molecular weight cutoff: 10,000) for 3 days. After dialysis, the polymer solution was filtered through a porous PTFE membrane (average pore size: 0.22 μm), and the product was isolated by evaporation of the methanol (yield: 78

%). ^{1}H NMR ($CDCl_3$, 600 MHz, ppm.): δ 7.84 (s, 2H, Ar-H), 7.67~7.70 (d, 4H, Ar-H), 4.00 (m, 8H, -O-C$\underline{H_2}$-), 2.13 (m, 4H, -C$\underline{H_2}$-), 1.55 (m, 4H, -C$\underline{H_2}$-), 1.41 (m, 4H, -C$\underline{H_2}$-), 1.23~1.30 (m, 12H, -C$\underline{H_2}$-, -C$\underline{H_3}$), 0.81 (m, 4H, -C$\underline{H_2}$-). ^{31}P NMR ($CDCl_3$, 600 MHz, ppm.): δ 32.95. Anal. Calcd. For $C_{31}H_{46}O_6P_2$: C, 64.57 %; H, 8.04 %. Found: C, 62.28 %; H, 8.01 %.

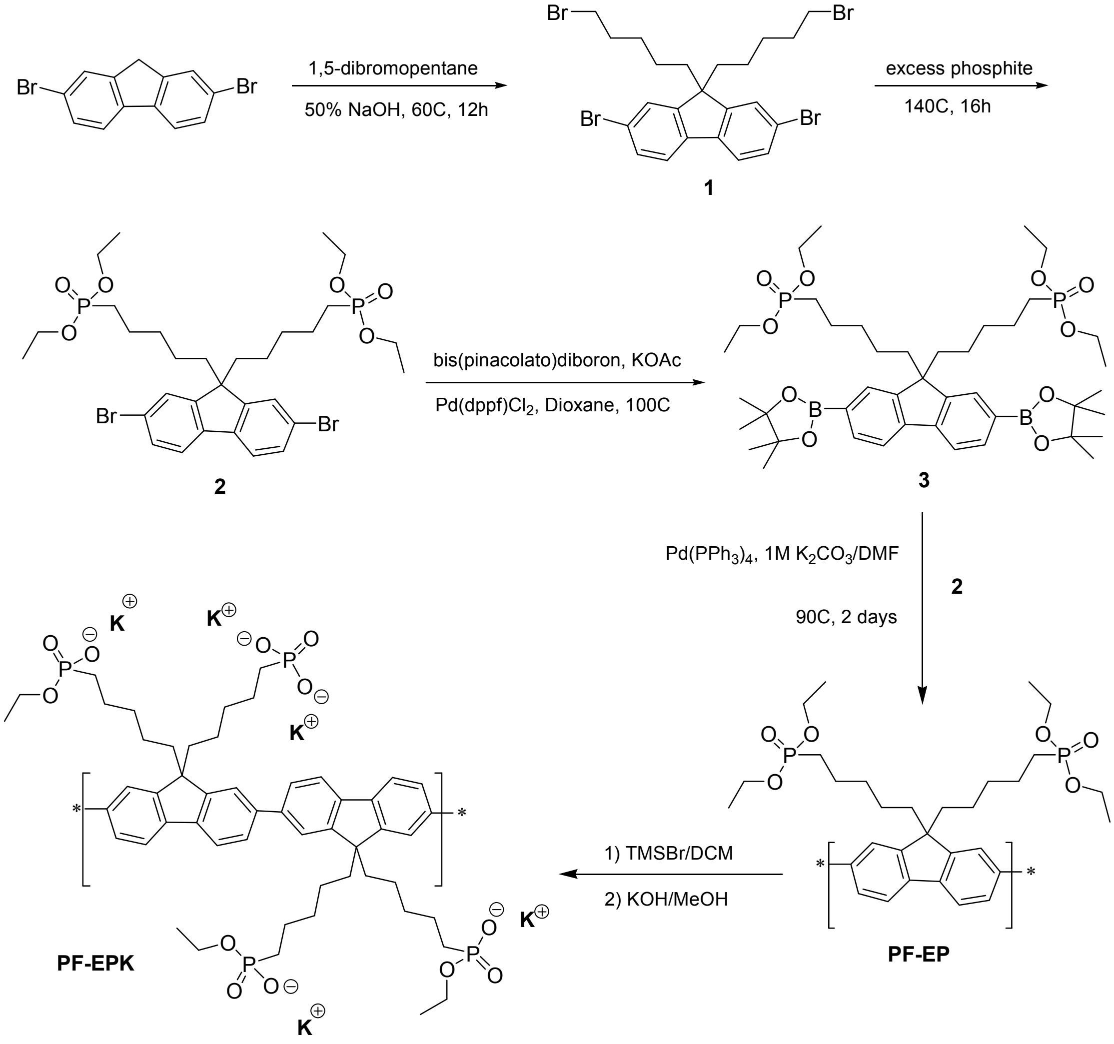

Scheme 1. Synthesis of **PF-EP** and **PF-EPK**.

Poly[9,9-bis(5'-phosphatepentyl)-fluorene] partially hydrolyzed (PF-EPK)

As shown in Scheme 1, the dealkylation of phosphonate groups in **PF-EP** (30 mg) was conducted in dichloromethane (5 ml) containing appropriate amount of bromotrimethylsilane (50 mg). The resulting solution was stirred at room temperature for 9 hours and then hydrolyzed by the addition of a mixture of 10 ml of methanol and 5 M aqueous KOH. The resulting solution was dialyzed against water using a cellulose membrane (molecular weight cutoff: 3500) for 1 day, and the **PF-EPK** was isolated by evaporation of the water (yield: 51 %). ^{1}H NMR (D_2O, 600 MHz, ppm.): δ 7.95 (m, 6H, Ar-H), 3.37 (m, 8H, -O-C$\underline{H_2}$-), 0.09~2.17 (m, 32H, -C$\underline{H_2}$-, -C$\underline{H_3}$).^{31}P NMR (D_2O, 600 MHz, ppm.): δ 35.11, 29.32, 23.81.

Results and Discussion

Synthesis and Characterization of PF-EP and PF-EPK

The polymer **PF-EP** was synthesized by the Suzuki-coupling of monomers **2** and **3** with $Pd(PPh_3)_4$ as the catalyst and K_2CO_3 as the base (Scheme 1). 2,7-dibromo-9,9-bis(5'-diethoxylphosphorylhexyl)-fluorene (**2**) was prepared according to the procedure reported previously[15], which in turn underwent Suzuki-Miyaura coupling with the pinacol ester of diboron to give 2,7-bis(4,4,5,5-tetramethyl-1,3,2-dioxaborolan-2-yl)-9,9-bis(5'-diethoxyl-phosphoryl pentyl)fluorene (**3) (**Supporting Information**)**. The novel conjugated polyelectrolyte (**PF-EPK**), with potassium ion as counter ion, was obtained from **PF-EP** via successive dealkylation with bromotrimethylsilane and partially hydrolyzed by KOH. The **PF-EPK** is soluble in high polar solvent such as water due to the hydrolyzed phosphonate groups, but the **PF-EP** is only soluble in common organic solvents. The chemical structures of **PF-EP** and **PF-EPK** were characterized by ^{1}H and ^{31}P NMR spectra. Their thermal decomposition temperatures were studied by the thermogravimetric analysis (TGA) to estimate hydrolysis ratio of pendant phosphonate groups.

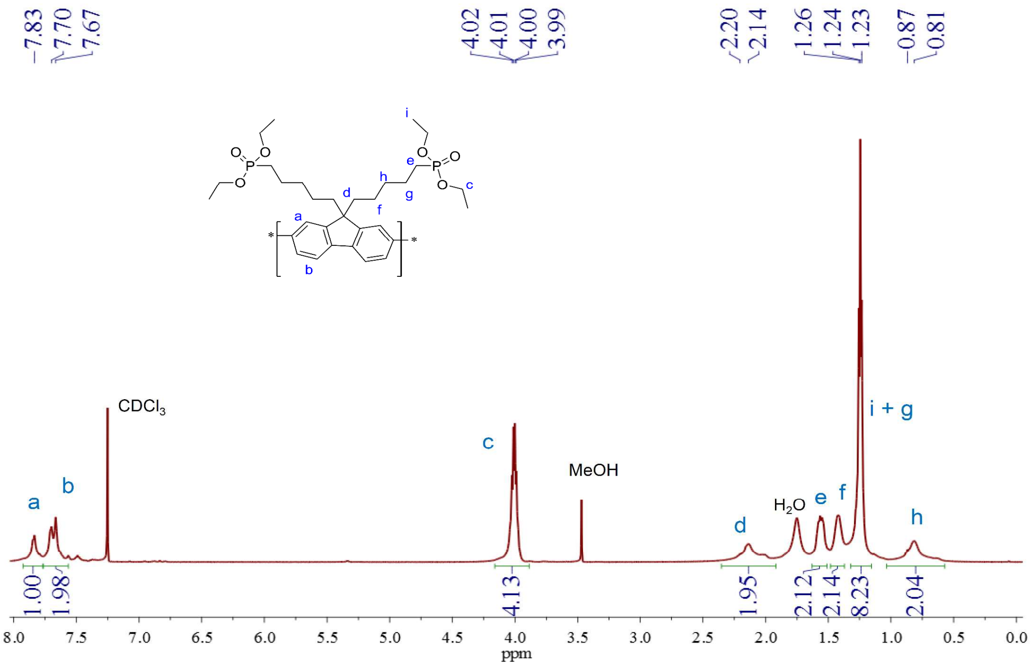

Figure 1. ^{1}H-NMR spectrum of **PF-EP**.

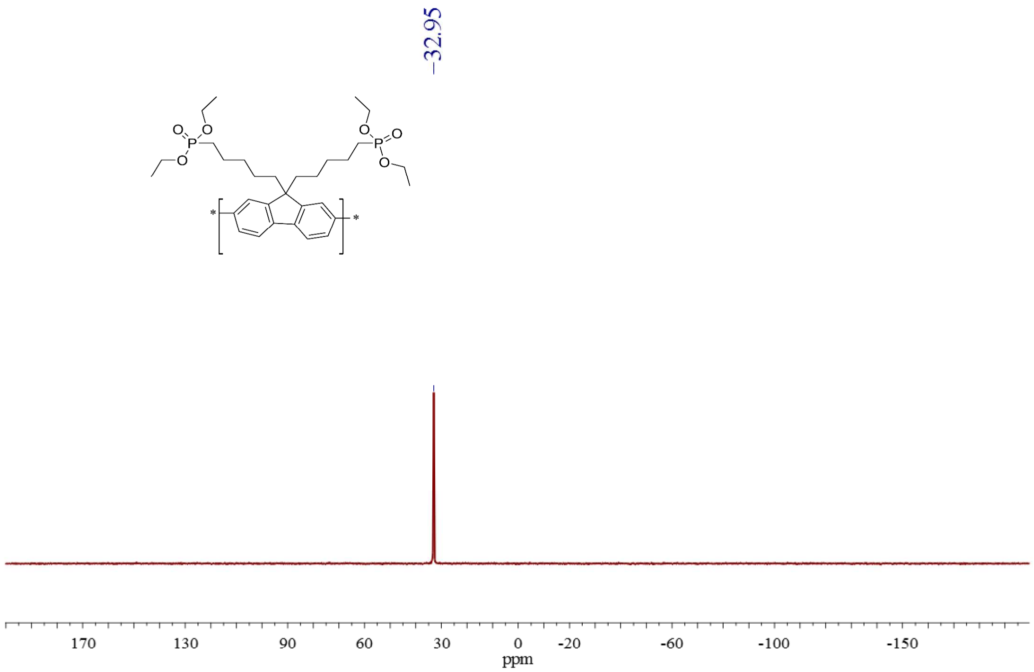

Figure 2. ^{31}P-NMR spectrum of **PF-EP**.

The chemical shifts at 2.20~0.81 ppm are attributed to the protons on the long pentylene spacers (d-h) and terminal methyl groups (i) of pendant phosphonates s in **PF-EP** (Figure 1). The aromatic protons in polyfluorene main chain are located at 7.83~7.67 ppm and the characteristic chemical shift of phosphonate groups are at around 4.00 ppm, attributed to the protons (c) attached to oxygen atom. The ^{31}P NMR of **PF-EP** showed only chemical shift at 32.95 ppm originated from pendant phosphonate groups (Figure 2). However, the ^{1}H NMR peaks of **PF-EPK** with the partially hydrolyzed phosphonate groups are much broader than those of **PF-EP** with slight shift (Figure 3). This is attributed to that the static repulsion between hydrolyzed phosphonate groups not only changes the chemical environment slightly but also extends polymer chain to result in more rigid structure. The chemical shifts at around 8.00 ppm are attributed to polyfluorene main chain and the characteristic chemical shifts at 3.70 ppm are assigned to protons attached to oxygen atom. The chemical shifts at 2.17~0.09 ppm are ascribed to the pentylene spacers and residual methyls on the pendant groups. The ^{31}P NMR of **PF-EPK** demonstrates two main chemical shifts (Figure 4), implying that there are two different phosphorus signals. The chemical shifts are located at 23.81 ppm and 29.32 ppm respectively, which depend on the degree of hydrolysis. The fully hydrolyzed **PF-EPK** with heavy electron cloud on oxygen atoms gives the upfield chemical shift; on the contrary, the signal shift to downfield regions.

Using the characteristic chemical shift of phosphonate groups at around 4.00 ppm, the amount of hydrolysis was estimated by peak area ratios of phosphonate groups to polyfluorene main chain. The ratio between phosphonate groups and the normalized aromatic peak area of **PF-EP** is 4.13/(1+1.98) = 1.39 (Figure 1). Therefore, the ratio of phosphonate groups of **PF-EP** and **PF-EPK** to the normalized aromatic peak area of their main chain is 1.39/0.44. Therefore, **PF-EPK** contains *ca.* 32% un-hydrolyzed phosphonate groups.

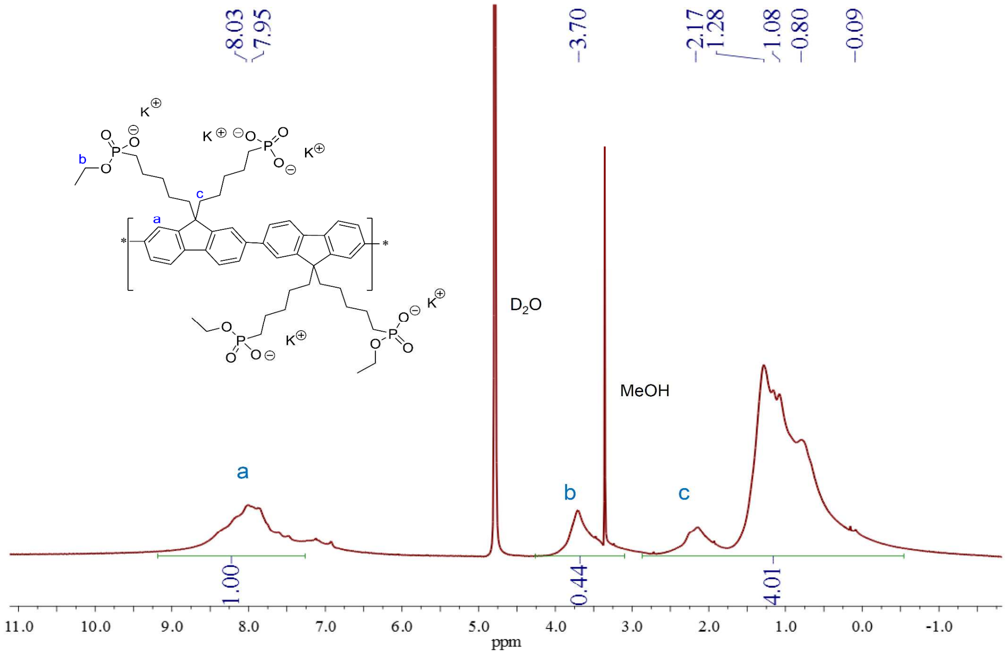

Figure 3. ^{1}H-NMR spectrum of **PF-EPK** in D_2O. (should be no peak for D_2O)

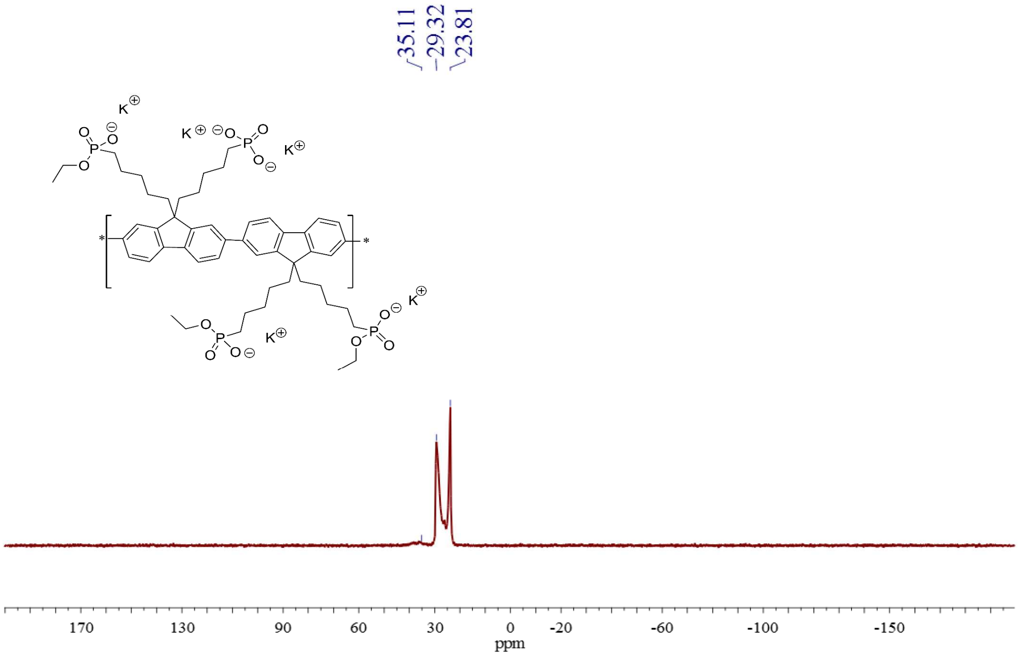

Figure 4. ^{31}P-NMR spectrum of **PF-EPK**.

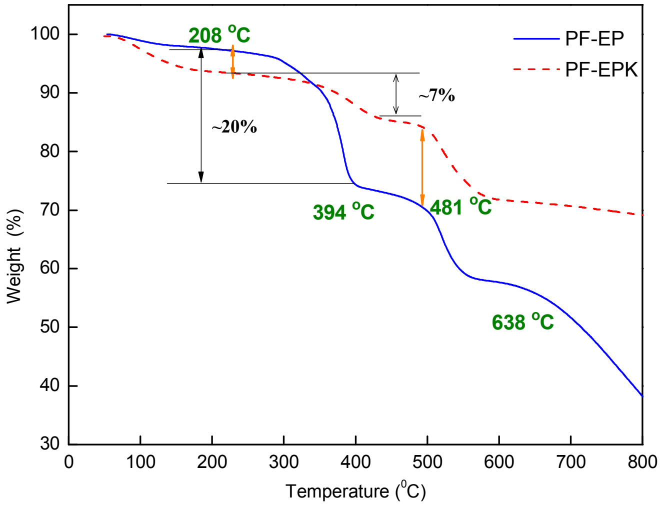

Figure 5. Thermo-gravimetric curves of **PF-EP** and **PF-EPK** at a heating rate of 10 C/min under nitrogen.

To further estimate the degree of hydrolysis of **PF-EPK**, quantitative loss of ethyl groups per repeating unit during thermal degradation was investigated by thermogravimetric analysis (TGA).[16] Both **PF-EPK** and **PF-EP** demonstrate three steps degradation in TGA thermograms (Figure 5), representing thermal decomposition of the ethyl groups in phosphonate groups, the long pentylene spacers and the main chains, respectively as shown in Figure 5. A moderate weight loss (about 3-4%) starts from 100 ^{o}C, which is obviously due to the release of associated water, **PF-EPK** and **PF-EP** exhibit the first-step degradation from 208 to 394 ^{o}C. The weight loss of **PF-EP** and **PF-EPK** are about 20 and 7 wt% respectively, which correspond to the quantity of un-hydrolyzed phosphonate groups per repeating unit. The 7 wt% loss of **PF-EPK** corresponded to 35% un-hydrolyzed phosphonate groups. The molar ratio of potassium ion and the organic part of **PF-EPK** is 2.7 to 1, which implies 2.7 potassium ions per repeating unit and *ca.* 67.5% phosphonate groups have been hydrohyzed. From the results of ^{1}H NMR and TGA, the amount of hydrolysis of **PF-EPK** was *ca.* 65~70%.

Electrochemical Properties

Cyclic voltammetry has been applied and considered as an effective tool to investigate electrochemical properties of conjugated polymers. A glassy carbon coated with **PF-EPK** or **PF-EP** were used as the working electrode and a solution of tetra-*n*-butylammonium perchlorate (Bu_4NClO_4: 0.1 M) in anhydrous acetonitrile was used as the electrolyte. The onset oxidation potentials of **PF-EPK** and **PF-EP** located at around 1.2 eV, whereas the reduction potentials situate at about -2.1 eV (Figure 6, Table 1). The highest occupied molecular orbital (HOMO) and lowest unoccupied molecular orbital (LUMO) levels were estimated by using the equations $E_{HOMO} = -(E_{ox} + 4.8)$ eV and $E_{LUMO} = -(E_{red} + 4.8)$ eV, where E_{ox} and E_{red} are the onset reduction and oxidation potentials, respectively, relative to the ferrocene/ferrocenium couple. The HOMO and LUMO energy levels of **PF-EP** are -5.53 eV and -2.25 eV respectively, and those of **PF-EPK** are -5.51 eV and -2.20 eV. Clearly, **PF-EP** and **PF-EPK** demonstrate almost identical HOMO and LUMO levels due to their polyfluorene backbone and similar pendent groups. In addition, compared with the HOMO (-5.8 eV) level of PFO,[15] the higher HOMO levels of **PF-EPK** (-5.51 eV) and **PF-EP** (-5.53 eV) should be attributed to the effect of pendant groups of polymer.[17]

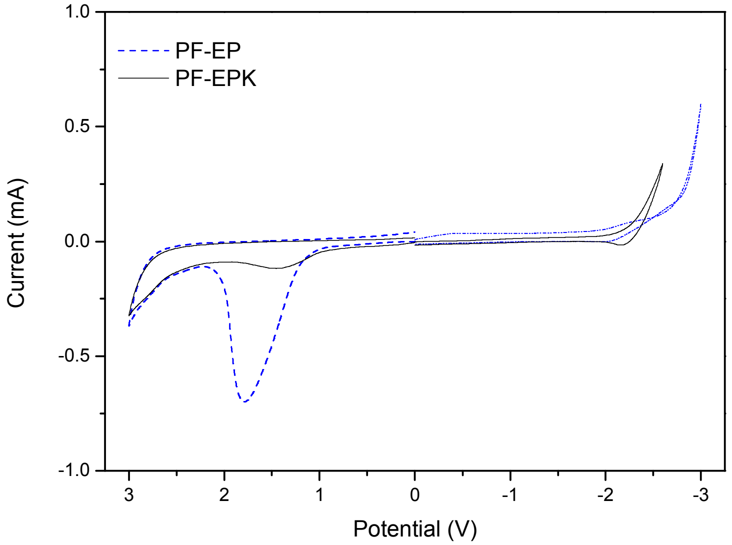

Figure 6. Cyclic voltammogram of **PF-EP** and **PF-EPK** in 0.1 M n-Bu_4NClO_4; scan rate: 100 mV/s.

Table 1. Electrochemical potentials of polymers.

Polymer	$E_{onset(ox)}$ *vs.* FOC(V)[a]	$E_{onset(red)}$ *vs.* FOC(V)[a]	E_{HOMO} (eV)[b]	E_{LUMO} (eV)[b]	E_g^{el} (eV)[c]
PF-EP	0.73	-2.55	-5.53	-2.25	3.28
PF-EPK	0.71	-2.60	-5.51	-2.20	3.31

---

[a] E_{FOC}= 0.47 V vs. Ag/AgCl.

[b] E_{HOMO}= -($E_{onset(ox)}$, FOC + 4.8) eV; E_{LUMO} = -($E_{onset(red)}$, FOC + 4.8) eV.

[c] Electrochemically-determined band-gap: E_g = |LUMO – HOMO|.

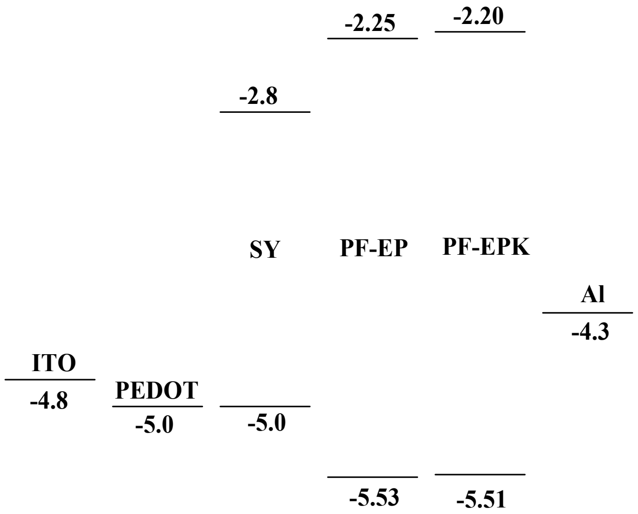

Figure 7. The energy band diagram of SY and **PF-EP**/**PF-EPK**.

Electroluminescent Properties

According to the energy band diagrams depicted in Figure 7, the energy barriers between aluminum (A1) and **PF-EPK** (2.05 eV) or **PF-EP** (2.10 eV) are larger than that between A1 and active layer, SY (1.5 eV). However, the enhancement of the electron injection/transport is due to the tunneling effect of **PF-EPK** and **PF-EP**. The phosphonate groups have a strong coordinating power to metal cathodes (Al) that results in the formation of an ultrathin interfacial layer (interfacial dipole and P–O–Al coordination), which can facilitate efficient electron injection from the cathodes.[18] Due to limited solubility of neat **PF-EPK** in methanol/water (19:1 v/v), which is good solvent for **PF-EP**, we tried blends of **PF-EPK** and **PF-EP** as electron-injection layer (EIL). Because of their similar chemical structures blending **PF-EPK** and **PF-EP** as electron-injection layer has been successfully applied to fabricate multi-layer polymer light-emitting diodes (PLEDs) by solution processes.

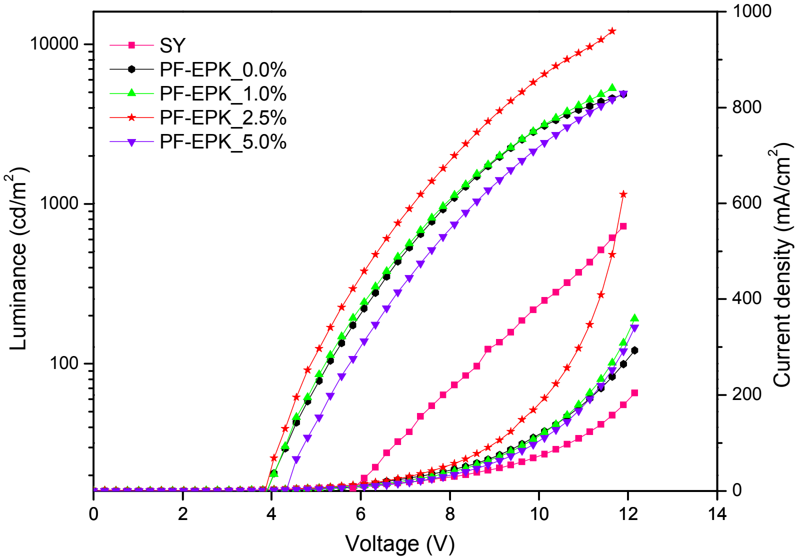

Figure 8. Luminance (L)-voltage (V)-current density (J) characteristics of PLEDs [ITO/PEDOT:PSS/SY/**PF-EP+PF-EPK**/Al].

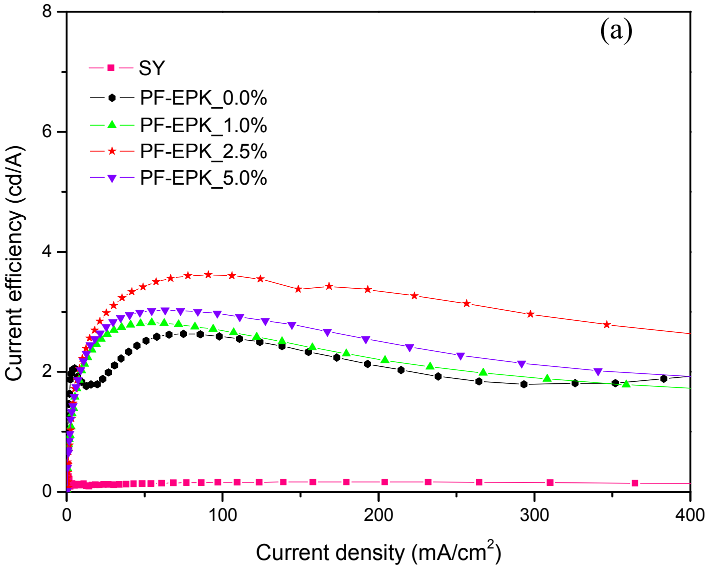

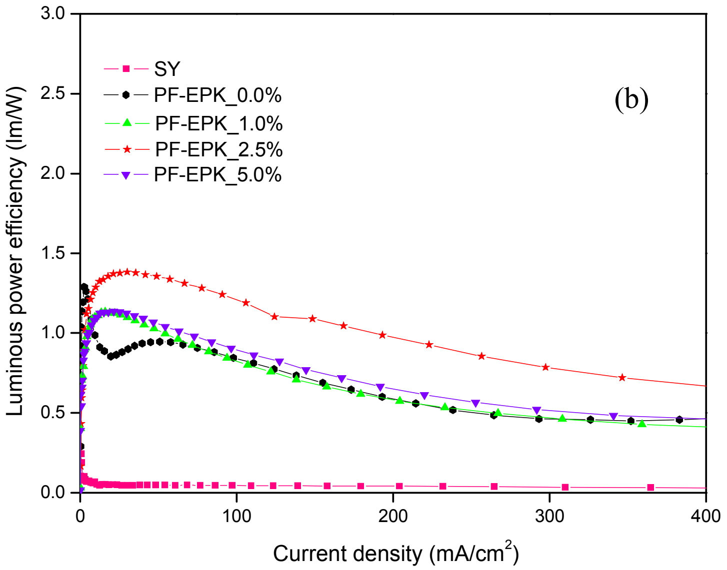

Figure 9. Current efficiency (a) and luminous power efficiency (b) versus current density characteristics of PLEDs [ITO/PEDOT:PSS/SY/**PF-EP+PF-EPK**/Al].

Table 2. Optoelectronic properties of the light-emitting diodes[a]

EIL	V_{on} (V)[b]	L $_{max}$ (cd/m^2)[c]	CE$_{max}$ (cd/A)[d]	LPE$_{max}$ (lm/W)[e]	CIE (x, y)[f]
None	5.3	725	0.16	0.05	(0.44, 0.55)
PF-EPK_0.0 %	3.8	4869	2.63	0.93	(0.45, 0.54)
PF-EPK_1.0 %	3.7	5292	2.82	1.13	(0.44, 0.54)
PF-EPK_2.5 %	3.5	12052	3.62	1.38	(0.44, 0.55)
PF-EPK_5.0 %	3.9	4925	3.01	1.14	(0.45, 0.54)

[a] Device structure: ITO/PEDOT:PSS/SY/EIL(**PF-EP**+**PF-EPK**)/Al

[b] Turn-on voltage at 10 cd/m^2.

[c] Maximum luminance.

[d] Maximum current efficiency.

[e] Maximum luminous power efficiency.

[f] The 1931 CIE coordinates at maximum luminance.

Multi-layer polymer light-emitting diodes (PLEDs) with a configuration of ITO/PEDOT:PSS/EML/(**PF-EP**+**PF-EPK**)/Al were fabricated, using blends of **PF-EP** and **PF-EPK** as electron-injection layer (EIL) and commercially available Superyellow (SY) (EL emission centered at 560 nm)[19] as emission layer (EML), to investigate their electroluminescent characteristics. Since **PF-EP** and **PF-EPK** are soluble in methanol containing a small amount of water, detrimental interface mixing between EML and EIL could be avoided during spin-coating of the EIL. Current density–luminance–voltage (J–L–V), luminous efficiency–power efficiency–current density (LE–PE–J), and electroluminescence (EL) spectra characteristics of the devices are shown in Figures 8-10, with the corresponding optoelectronic data summarized in Table 2.

Electroluminescent performances are apparently enhanced by inserting the electron-injection layer between emitting layer (SY) and Al cathode (Figure 8-9 and Table 2). Maximum luminance and current efficiency of devices with inserting the electron-injection layer (EIL: neat **PF-EP**) between emitting layer (SY) and Al cathode were effectively enhanced to 4869 cd/m^2 and 2.63 cd/A from 725 cd/m^2 and 0.16 cd/A of the device without EIL, respectively. The performance enhancement is attributable to improved electron injection/transport in the presence of EIL that leads to higher charges recombination ratio.

The device performances are significantly enhanced in blending of **PF-EPK** into **PF-EP** with different concentration (1.0 wt%, 2.5 wt%, and 5.0 wt%). The best performance was obtained for the device with (**PF-EP** + 2.5% **PF-EPK)** as EIL. The maximum luminance, maximum current efficiency and maximum luminous power efficiency were further significantly enhanced to 12052 cd/m^2, 3.62 cd/A, and 1.38 lm/W, respectively. However, design concept of our **PF-EPK** containing partially hydrolyzed phosphonate groups with potassium ion is different from that of the thermo-cleavable materials crosslinked through a hydrogen-bonded network and coordination of O, P and Li.[16] As shown in Figure 8, the curve shifts horizontally to lower bias as **PF-EPK**'s ratio is increased from 0 to 2.5%. The horizontal shift means the current density is enhanced under the same bias. For instance, the current density increases from ca. 100 mA/cm^2 to ca. 200 mA/cm^2 at a bias of 10V, due to increased electron transport at high **PF-EPK** contents. In addition, the turn-on voltage of the device with EIL (**PF-EP** + 2.5% **PF-EPK)** was decreased to 3.5 V which is much lower than 5.3 V obtained for that without EIL (Table 2). In addition, the increased current density and reduced turn-on voltage indicate that blending trace **PF-EPK** into **PF-EP** as EIL have greatly improved the electron injection/transport abilities. Therefore, the blends of **PF-EP** and **PF-EPK** as electron-injection layer (EIL) effectively promoted electron injection/transport to significantly enhance the device performance. The electroluminescent emission of all devices is exclusively originated from emitting layer (SY), with full width at half-maxima (fwhm) being *ca*. 80 nm (Figure 10). The 1931 CIE coordinates (x, y) of the EL emission only shift slightly from (0.44, 0.55) of neat SY-based device to (0.45, 0.54) of devices with EIL **(PF-EP** + 5.0% **PF-EPK**) (Figure 10 and Table 2).

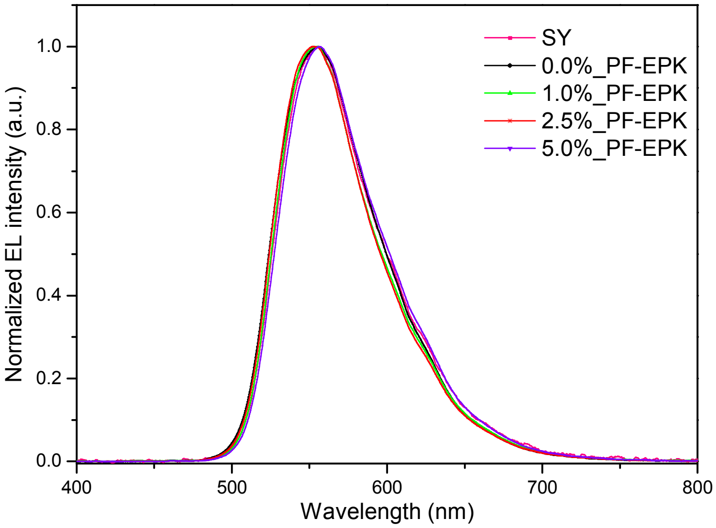

Figure 10. The normalized EL spectra of the EL devices at maximum luminance [ITO/PEDOT:PSS/SY/**PF-EP**+**PF-EPK**/Al].

The devices with **PF-EPK**-blended EILs exhibited much better performances than **PF-EP** (Figure 8-9 and Table 2). However, further increase in **PF-EPK** content to 5.0 wt% leads to quick degradation in maximum luminance and maximum current efficiency (diminish to 4925 cd/m^2 and 3.01 cd/A respectively). To elucidate this performance degradation at 5.0 wt% **PF-EPK** and to demonstrate the electron-injection ability of the EILs [neat **PF-EP** and blends of **PF-EP** with various ratios of **PF-EPK**], photovoltaic (PV) measurements were conducted to determine open-circuit voltages (V_{oc}s) of the PLEDs. The V_{oc} is an effective value to evaluate electron-injection ability of PLEDs. Figure 11 and Table 3 reveals that neat **PF-EP** and blends of **PF-EP** with **PF-EPK** increase V_{oc} greatly depending on the contents of **PF-EPK**, indicating that they play crucial role in promoting electron-injection in the PLEDs.

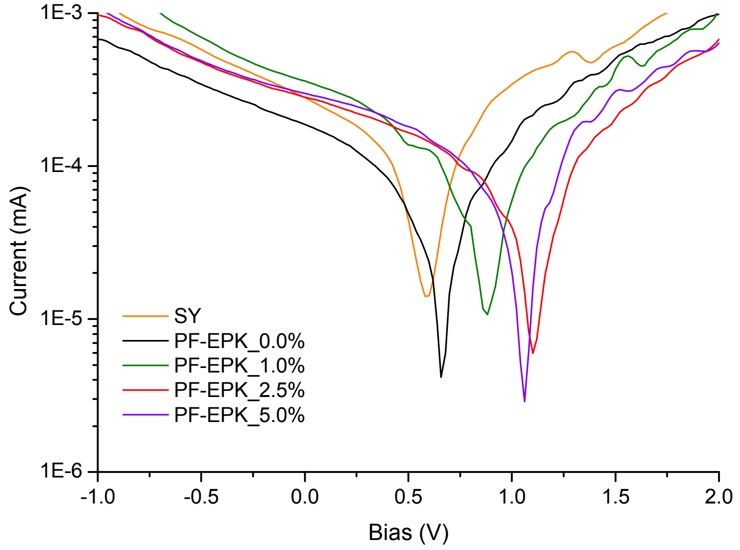

Figure 11. Photovoltaic characteristics of devices with different EIL (ITO/PEDOT:PSS/SY/EL (**PF-EP+PF-EPK**)/Al).

Table 3. Photovoltaic properties of the light-emitting diodes.[a]

EIL[b]	None	**PF-EP**	**PF-EP** + 1.0 % **PF-EPK**	**PF-EP** + 2.5 % **PF-EPK**	**PF-EP** + 5.0 % **PF-EPK**
V_{oc}[c](V)	0.64	0.66	0.88	1.10	1.06

[a] Device structure: ITO/PEDOT:PSS/SY/EIL/Al

[b] Electron injection layer, EIL.

[c] Open-circuit voltage.

When the anode is kept identical (ITO/PEDOT:PSS), the open-circuit voltage (V_{oc}) is primarily determined by effective work-function of the cathode, which reflects the electron-injection ability of the EIL materials.[20] The improved device performance has been attributed to enhanced electron-injection ability through cathode modification by the EIL. The V_{oc} was 0.64 V for the device based on SY without EIL, which was slightly increased to 0.66 V when neat **PF-EP** was inserted as the EIL. The V_{oc}s were further raised to 0.88 V, 1.10 V and 1.06 V when blends of **PF-EP** with various ratios of **PF-EPK** (1.0 wt%, 2.5 wt%, and 5.0 wt%) were used as EIL, respectively. Higher V_{oc} means that the built-in potential (the difference in work-function between anode and cathode) across its anode/EML/cathode junction has been increased. Moreover, the highest V_{oc} (1.10 V) corresponds to the best device performances for the devices using **PF-EP** with 2.5 wt% **PF-EPK**, but slightly decreased to 1.06 V at 5 wt% **PF-EPK**. This indicates that the electron-injection ability is greatly improved upon blending **PF-EPK**, the optimal amount is 2.5% **PF-EPK** in terms of device performance.

In order to investigate the morphology of polymer films, the atomic force microscopy (AFM) was used to examine the surface roughness of the EILs [neat **PF-EP** and blends of **PF-EP** with various ratios of **PF-EPK** (1.0 wt%, 2.5 wt%, and 5.0 wt%)] (Figure 12, Table 4). The AFM images of neat **PF-EP** film show higher roughness (rms roughness: 1.98 nm) than that based on SY without EIL (1.69 nm). Moreover, when blends of **PF-EP** with various amount of **PF-EPK** as EIL, the surfaces roughness also became rougher and their rms roughness reached to 3.81~4.43 nm. However, the device with 2.5 wt% **PF-EPK** showed highest surface roughness (4.43 nm) and exhibited the best device performance (12052 cd/m^2, 3.62 cd/A, and 1.38 lm/W). Moreover, the highest V_{oc} (1.10 V) corresponds to the best device performances for the devices using **PF-EP** with 2.5 wt% **PF-EPK**. This is probably attributed to the higher surface roughness to increase the contact area between EIL and metal cathode;[21] however, optimal amount of **PF-EPK** (2.5 wt%) is also an important factor in promoting electron injection effectively.

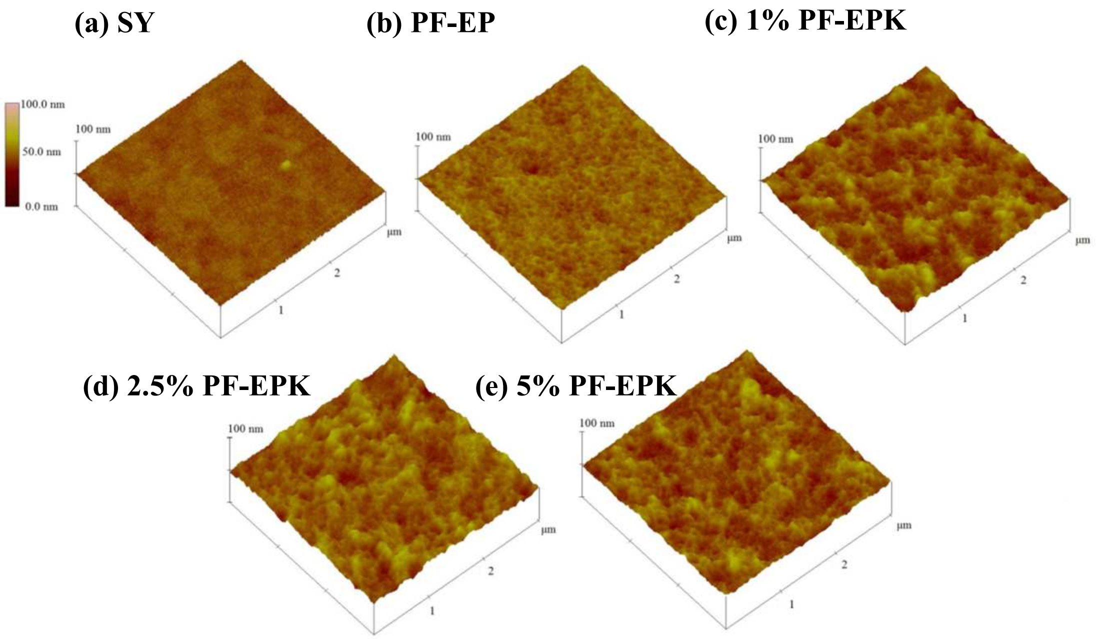

Figure 12. AFM images of different films spin-coated on top of SY layer. (a) None, (b) **PF-EP**, (c) **PF-EP** doped with 1.0 % **PF-EPK**, (d) **PF-EP** doped with 2.5 % **PF-EPK**, (e) **PF-EP** doped with 5.0 % **PF-EPK**.

Table 4. Surface morphology of different films spin-coated on top of SY.

Films	None	**PF-EP**	**PF-EP** + 1.0 % **PF-EPK**	**PF-EP** + 2.5 % **PF-EPK**	**PF-EP** + 5.0 % **PF-EPK**
rms roughness[a]	1.69	1.98	4.15	4.43	3.81

[a] Surface root mean square (rms) roughness.

Conclusion

Poly[9,9-bis(5'-diethoxylphosphorylpentyl)-fluorene] **(PF-EP)** was synthesized by Suzuki coupling reaction and partially hydrolyzed with bromotrimethylsilane and KOH to give a novel conjugated polyelectrolyte **PF-EPK** for application as electron-injection layer (EIL) in polymer light-emitting diodes (PLEDs). The amount of hydrolysis was estimated to be about 65-70%, by comparing the ^{1}H NMR and TGA of **PF-EPK** with those of **PF-EP**. Multilayer PLEDs (ITO/PEDOT:PSS/EML/**PF-EP**+**PF-EPK**/Al) with **PF-EP** doped with 2.5% **PF-EPK** as EIL exhibited the optimal performance. The maximum luminance, maximum current efficiency and maximum luminous power efficiency were 12052 cd/m^2, 3.62 cd/A and 1.38 lm/W, respectively, which were obviously superior to those without the EIL (725 cd/m^2, 0.16 cd/A, 0.05 lm/W). The enhancement in electron-injection ability through cathode modification by the EIL was confirmed by photovoltaic measurements and the device with 2.5 wt% **PF-EPK** showed the maximum open-circuit voltage (V_{oc}). In addition, the device with 2.5 wt% **PF-EPK** showed highest surface roughness (4.43 nm) and exhibited the best device performance (12052 cd/m^2, 3.62 cd/A, and 1.38 lm/W) which is due to the increase in contact area. These results indicated that **PF-EPK** is a promising electron-injection material for optoelectronic devices.

Supporting Information

Synthesis and characterization of monomers 1-3.

Acknowledgment

This research received funding from the Headquarters of University Advancement at the National Cheng Kung University, which is sponsored by the Ministry of Education, Taiwan, ROC.

References and Notes

[1] Burroughes, J. H.; Bradley, D. D. C.; Brown, A. R.; Marks, R. N.; Mackay, K.; Friend, R. H.; Burns, P. L.; Holmes, A. B., *Nature* 1990, **347**, 539.

[2] Sheats, J. R.; Antoniadis, H.; Hueschen, M.; Leonard, W.; Miller, J.; Moon, R.; Roitman, D.; Stocking, A., *Science* 1996, **273**, 884.

[3] Friend, R. H.; Gymer, R. W.; Holmes, A. B.; Burroughes, J. H.; Marks, R. N.; Taliani, C.; Bradley, D. D. C.; Dos Santos, D. A.; Bredas, J. L.; Logdlund, M.; Salaneck, W. R., *Nature* 1999, **397**, 121.

[4] Adachi, C.; Tsutsui, T.; Saito, S., *Appl Phys Lett* 1990, **57**, 531.

[5] OBrien, D.; Bleyer, A.; Lidzey, D. G.; Bradley, D. D. C.; Tsutsui, T., *J Appl Phys* 1997, **82**, 2662.

[6] Huang, F.; Wu, H. B.; Cao, Y., *Chem Soc Rev* 2010, **39**, 2500.

[7] Huang, F.; Cheng, Y. J.; Zhang, Y.; Liu, M. S.; Jen, A. K. Y., *J Mater Chem* 2008, **18**, 4495.

[8] Muller, C. D.; Falcou, A.; Reckefuss, N.; Rojahn, M.; Wiederhirn, V.; Rudati, P.; Frohne, H.; Nuyken, O.; Becker, H.; Meerholz, K., *Nature* 2003, **421**, 829.

[9] Veinot, J. G. C.; Marks, T. J., *Accounts Chem Res* 2005, **38**, 632.

[10] Huang, F.; Shih, P. I.; Shu, C. F.; Chi, Y.; Jen, A. K. Y., *Adv Mater* 2009, **21**, 361.

[11] (a) Wu, H. B.; Huang, F.; Mo, Y. Q.; Yang, W.; Wang, D. L.; Peng, J. B.; Cao, Y., *Adv Mater* 2004, **16**, 1826. (b) Jin, S. H.; Kim, M. Y.; Kim, J. Y.; Lee, K.; Gal, Y. S., *J Am Chem Soc* 2004, **126**, 2474.

[12] (a) Wu, C.-S.; Chen, Y. *Macromolecules* **2009**, 42, 3729. (b) Wu, C.-S.; Chen, Y. *J. Mater. Chem.* **2010**, 20, 7700. (c) Wu, C.-S.; Chen, Y. *J. Polym. Sci. Part*

A Polym. Chem. **2010**, 48, 5727. (d) Wu, C.-S.; Lee, S.-L.; Chen, Y. *J. Polym. Sci. Part A Polym. Chem.* **2011**, 49, 3099. (e) Wu, C.-S.; Chen, Y. *J. Polym. Sci. Part A Polym. Chem.* **2011**, 49, 3928. (f) Wu, C.-S.; Yang, Y.-J.; Fang, S.-W.; Chen, Y. *J. Polym. Sci. Part A Polym. Chem.* **2012**, 50, 3875. (g) Wu, C.-S.; Lee, Y.-T.; Chen, Y. *Polym. Chem.* **2012**, 3, 2776. (h) Wu, C.-S.; Liu, C.-T.; Chen, Y. *Polym. Chem.*, **2012**, 3, 3308. (i) Wu, C.-S.; Wu, J.-W.; Chen, Y. *J. Mater. Chem.* **2012**, 22, 23877. (j) Wu, C.-S.; Fang, S.-W.; Chen, Y. *Phys. Chem. Chem. Phys.* **2013**, 15, 15121. (k) Wu, C.-S.; Chen, C.-P.; Chen, Y. *J. Polym. Sci. Part A Polym. Chem.* **2013**, 51, 3975. (l) Wu, C.-S.; Lu, H.-A.; Lin, Y.-J.; Chen, Y. *J. Mater. Chem. C* **2013**, 1, 6850. (m) Wu, C.-S.; Lin, Y.-J.; Chen, Y. *Org. Biomol. Chem.* **2014**, 12, 1419. (n) Wu, C.-S.; Lu, H.-A.; Chen, C.-P.; Guo, T.-F.; Chen, Y. *Org. Biomol. Chem.,* **2014**, 12, 1430. (o) Wu, C.-S.; Wu, Y.-S.; Chen, Y. *Phys. Chem. Chem. Phys.* **2014**, 16, 8927.

[13] Huang, J. S.; Li, G.; Wu, E.; Xu, Q. F.; Yang, Y., *Adv Mater* 2006, **18**, 114.

[14] Piromreun, P.; Oh, H.; Shen, Y. L.; Malliaras, G. G.; Scott, J. C.; Brock, P. J., *Appl Phys Lett* 2000, **77**, 2403.

[15] Zhou, G.; Qian, G.; Ma, L.; Cheng, Y. X.; Xie, Z. Y.; Wang, L. X.; Jing, X. B.; Wang, F. S., *Macromolecules* 2005, **38**, 5416.

[16] Ye, T. L.; Zhu, M. R.; Chen, J. S.; Fu, Q.; Zhao, F. C.; Shi, C. S.; Hu, Y.; Ma, D. G.; Yang, C. L., *J Mater Chem* 2012, **22**, 6413-6418.

[17] Huang, F.; Wu, H. B.; Wang, D.; Yang, W.; Cao, Y., *Chem Mater* 2004, **16**, 708.

[18] Zhang, B. H.; Xie, Z. Y.; Wang, L. X., *Polym Bull* 2012, **68**, 829.

[19] Guo, T. F.; Yang, F. S.; Tsai, Z. J.; Wen, T. C.; Hsieh, S. N.; Fu, Y. S.; Chung, C. T., *Appl Phys Lett* 2006, **88**.

[20] (a) Xu, Q.; Quyang, J.; Yang Y.; Ito, T.; Kido, J., *Appl Phys Lett* 2003, **83**, 4695.

(b) Chen, F.-C.; Chien, S.-C.; Lee, S.-W., *Electrochem. Solid-State Lett.* 2008, **11(6)**, J50.

[21] Ma, W. L.; Iyer, P. K.; Gong, X.; Liu, B.; Moses, D.; Bazan, G. C.; Heeger, A. J., *Adv Mater* 2005, **17**, 274.